Numerical differentiation for local and global tangent operators in computational plasticity [*]

Agustí PÉREZ-FOGUET, Antonio RODRÍGUEZ-FERRAN
and Antonio HUERTA [1]

Departament de Matemàtica Aplicada III, E.T.S. de Ingenieros de Caminos
Edifici C2, Campus Nord, Universitat Politècnica de Catalunya
E-08034 Barcelona, Spain. web: `www.upc.es/ma3/lacan.html`

Abstract

In this paper, numerical differentiation is applied to integrate plastic constitutive laws and to compute the corresponding consistent tangent operators. The derivatives of the constitutive equations are approximated by means of difference schemes. These derivatives are needed to achieve quadratic convergence in the integration at Gauss-point level and in the solution of the boundary value problem. Numerical differentiation is shown to be a simple, robust and competitive alternative to analytical derivatives. Quadratic convergence is maintained, provided that adequate schemes and stepsizes are chosen. This point is illustrated by means of some numerical examples.

Key words: finite element method, consistent tangent operators, numerical differentiation, difference schemes, quadratic convergence.

1 INTRODUCTION

The main goal of this paper is to show that numerical differentiation is a useful tool for achieving quadratic convergence in computational plasticity. Two different problems must be solved: 1) the integration of the constitutive law at each Gauss point (the local problem) and 2) the boundary value problem (the global problem) [3,4].

---

[*] Partially supported by CICYT, Spain. Grant contract: TAP98-0421
[1] Corresponding author. e-mail: `huerta@lacan.upc.es`

If the constitutive law is integrated with an implicit method, the local problem is nonlinear. To solve it with the Newton-Raphson method (thus attaining quadratic convergence [3,5]), it is necessary to compute the Jacobian of the residual at the Gauss-point level.

The global problem, on the other hand, is typically solved via an incremental/iterative approach [3]. At each load increment, a nonlinear system of equations must be solved. To do it with the Newton-Raphson method and achieve quadratic convergence, the consistent tangent matrix (computed with the consistent elastoplastic moduli) must be used [21,25].

In both problems (local and global), the derivatives of the constitutive equation are needed. These derivatives are a key ingredient of both the Jacobian of the residual —local problem— and the consistent elastoplastic moduli —global problem.

Various approaches for computing these derivatives can be found in the literature. For simple plasticity models, analytical derivatives are readily available, and this leads to closed-form return mapping algorithms for the local problem and compact, explicit expressions of the consistent elastoplastic moduli for the global problem [3,23,25]. In more complicated models, analytical differentiation is rather more cumbersome. Algebraic manipulators such as Maple or Mathematica can be a very effective tool for obtaining analytical derivatives.

Here a different approach is proposed: derivatives are approximated by means of classical difference schemes [5,7,8]. The approximated derivatives are used both for the integration of the constitutive equations (local problem) and for the computation of the consistent tangent moduli (global problem). The resulting algorithm is both robust and computationally efficient. It maintains the characteristic quadratic convergence of the Newton-Raphson method, provided that adequate difference schemes and stepsizes (i.e. the perturbation in the difference scheme) are chosen.

Some applications of numerical differentiation to other problems of computational plasticity can be found in the literature. In Reference [14], for instance, a first-order forward difference scheme is used to compute the consistent tangent moduli needed in large-strain inelasticity. In [14] simple material models are used and closed expressions for the return mapping are available, so numerical derivatives are only applied to the global problem. The proposed numerical approach computes the derivatives of each stress component with respect to each strain component to get directly the consistent moduli. This implies a computational overhead (with respect to analytical derivatives) that ranges from 40% to 80% and, perhaps more importantly, its robustness is limited by the choice of the stepsize. In References [9,10] more complicated models are considered, but it is also concluded that analytical derivatives are clearly

superior to numerical derivatives regarding computational cost.

In constrast to these approaches, the strategy proposed here, concerned with small strains, combines the three following features: 1) it can be used for both local and global problems, with complicated material models [17], 2) it has a marginal computational overhead (around 1%-2%) and 3) it is very robust (i.e. insensitive to the choice of the stepsize).

An outline of this paper follows. The local and the global problems of computational plasticity are briefly reviewed in section 2, with emphasis on the crucial role of the derivatives of the constitutive equation. In section 3 the various numerical differentiation techniques are summarized, and a simple rule for selecting the stepsize is presented. These numerical approximations are applied to several problems in section 4. Finally, some concluding remarks are made on section 5. For the sake of simplicity, the simple case of a single yield surface and the backward Euler integration rule is considered. However, the same derivatives are needed in multisurface plasticity [19,24] or with other implicit integration rules [2,16,22], so numerical differentiation can also be applied in these general cases.

2 PROBLEM STATEMENT

In small strain elastoplasticity [23], the stress tensor $\boldsymbol{\sigma}$ and the stress-like internal variables $\mathbf{q}$ are related with the small strain tensor $\boldsymbol{\epsilon}$ and the strain-like internal variables $\mathbf{p}$ through

$$\boldsymbol{\sigma} = \nabla W(\boldsymbol{\epsilon}^e) = \nabla W(\boldsymbol{\epsilon} - \boldsymbol{\epsilon}^p) \quad \text{and} \quad \mathbf{q} = -\nabla \mathcal{H}(\mathbf{p}) \,, \qquad (1)$$

where $\boldsymbol{\epsilon}^e$ and $\boldsymbol{\epsilon}^p$ are the elastic and the plastic strain tensors, W and $\mathcal{H}$ are the elastic and the inelastic part of the free-energy function, and $\nabla \Psi(\chi)$ denotes the gradient of Ψ with respect to χ. The yield function F defines the admissible stress states, $F(\boldsymbol{\sigma}, \mathbf{q}) \leq 0$. Its derivatives are denoted by $\mathbf{n}_{\boldsymbol{\sigma}} = \partial F/\partial \boldsymbol{\sigma}$ and $\mathbf{n}_{\mathbf{q}} = \partial F/\partial \mathbf{q}$. The equations of evolution for $\boldsymbol{\epsilon}^p$ and $\mathbf{p}$ are

$$\dot{\boldsymbol{\epsilon}}^p = \dot{\lambda} \mathbf{m}_{\boldsymbol{\sigma}} \quad \text{and} \quad \dot{\mathbf{p}} = \dot{\lambda} \mathbf{m}_{\mathbf{q}} \,, \qquad (2)$$

where $\mathbf{m}_{\boldsymbol{\sigma}}$ and $\mathbf{m}_{\mathbf{q}}$ are the corresponding flow directions, and $\dot{\lambda}$ is the plastic consistency parameter. For convenience, the terms *generalized stress* and *generalized flow vector* are used to refer to $(\boldsymbol{\sigma}, \mathbf{q})$ and $(\mathbf{m}_{\boldsymbol{\sigma}}, \mathbf{m}_{\mathbf{q}})$ respectively [15,23]. For some constitutive models, the generalized flow vector is expressed as the derivative of a generalized flow potential $G(\boldsymbol{\sigma}, \mathbf{q})$ [11,20]: $\mathbf{m}_{\boldsymbol{\sigma}} = \partial G/\partial \boldsymbol{\sigma}$ and $\mathbf{m}_{\mathbf{q}} = \partial G/\partial \mathbf{q}$. The flow potential G may either coincide with (associate plasticity) or differ from (non-associate plasticity) the yield function F.

2.1 Local problem: integration of the constitutive law

The integration of the constitutive law with an implicit rule results in a non-linear problem. If the backward Euler rule is used, the equations are

$$^{n+1}\boldsymbol{\sigma} = \nabla W \left(^{n+1}\boldsymbol{\epsilon} - {}^{n}\boldsymbol{\epsilon}^{p} - {}^{n+1}\lambda\, {}^{n+1}\mathbf{m}_{\boldsymbol{\sigma}} \right) \tag{3}$$

$$^{n+1}\mathbf{q} = -\nabla \mathcal{H} \left(^{n}\mathbf{p} + {}^{n+1}\lambda\, {}^{n+1}\mathbf{m}_{\mathbf{q}} \right) \tag{4}$$

$$F(^{n+1}\boldsymbol{\sigma}, {}^{n+1}\mathbf{q}) = 0 \tag{5}$$

where the superscripts n and $n+1$ refer to instants t_n and $t_{n+1} = t_n + \Delta t$ respectively.

There are several ways to solve this nonlinear problem. For some very simple models, it can be solved analytically [3,23]. However, for general models an analytical solution is not possible, so a numerical method must be used. A typical choice is the Newton-Raphson method, because it converges quadratically [3,5]. To use this method, the derivatives of equations (3–5) with respect to the unknowns $^{n+1}\boldsymbol{\sigma}$, $^{n+1}\mathbf{q}$, and $^{n+1}\lambda$ are needed. With the standard vector notation of computational mechanics [30] and dropping the superscript $n+1$, this Jacobian is

$$\mathbf{J} = \begin{pmatrix} \mathbf{I} + \lambda \mathbf{E}\frac{\partial \mathbf{m}_{\boldsymbol{\sigma}}}{\partial \boldsymbol{\sigma}} & \lambda \mathbf{E}\frac{\partial \mathbf{m}_{\boldsymbol{\sigma}}}{\partial \mathbf{q}} & \mathbf{E}\mathbf{m}_{\boldsymbol{\sigma}} \\ \lambda \mathbf{H}\frac{\partial \mathbf{m}_{\mathbf{q}}}{\partial \boldsymbol{\sigma}} & \mathbf{I} + \lambda \mathbf{H}\frac{\partial \mathbf{m}_{\mathbf{q}}}{\partial \mathbf{q}} & \mathbf{H}\mathbf{m}_{\mathbf{q}} \\ \mathbf{n}_{\boldsymbol{\sigma}}^{T} & \mathbf{n}_{\mathbf{q}}^{T} & 0 \end{pmatrix} \tag{6}$$

where $\mathbf{E} = \nabla^2 W(\boldsymbol{\epsilon}^e)$ is the tensor of elastic moduli, $\mathbf{H} = \nabla^2 \mathcal{H}(\mathbf{p})$ is the tensor of plastic moduli and T denotes transpose. The expression of the Jacobian given in equation (6) can be compacted by multiplying the first row by $\mathbf{E}^{-1}$ and the second row by $\mathbf{H}^{-1}$ [23]. This transformation (which must, of course, also be performed on the RHS residual vector of the Newton-Raphson iteration) is computationally appealing if matrices $\mathbf{E}$ and $\mathbf{H}$ are constant. However, the ideas presented in this paper do not rely at all in this transformation. For this reason, the original expression of the Jacobian is retained here.

Of the terms in equation (6), the derivatives of the generalized flow vector with respect to the generalized stresses are usually the most difficult to compute. For complex material models, these derivatives are either not available or computationally too expensive [6,10,19,29]. The standard approach in these cases is to use nonlinear solvers (different from the Newton-Raphson method, i.e. a fully tangent approach) that do not need to compute all the derivatives of the generalized flow vector.

Some of these alternatives are: a tangent approach for the plastic multiplier,

equation (5), with an explicit expression for internal variables, equation (4), and a secant approach for stresses, equation (3) [19]; a tangent approach for the stresses, equation (3), and a direct substitution of the internal variable equations, equation (4) [9,10]; a two-level technique with a tangent approach for the stress invariants and a Picard iteration with an adaptive order inverse interpolation for the internal variables [13]. However, quadratic convergence cannot be achieved with these methods, because they are not based on a consistent linearization of *all* the equations and unknowns.

The goal of this paper is to show that numerical differentiation is a valid alternative to these approaches. By approximating numerically the derivatives of the generalized flow vector, the standard full Newton-Raphson method can be applied to equations (3–5). In this manner, quadratic convergence is obtained.

2.2 Global problem: the consistent tangent matrix

Various nonlinear solvers may be used for the global problem [3,5]. Again, one of the best choices is the full Newton-Raphson method. To achieve quadratic convergence, the consistent tangent matrix must be used [21,25]. To compute this matrix, the consistent tangent moduli $\mathrm{d}^{n+1}\boldsymbol{\sigma}/\mathrm{d}^{n+1}\boldsymbol{\epsilon}$ are needed. They can be computed by linearizing the discrete constitutive equations (3–5). This linearization can be represented as

$$\mathbf{J} \begin{pmatrix} \mathrm{d}\,^{n+1}\boldsymbol{\sigma} \\ \mathrm{d}\,^{n+1}\mathbf{q} \\ \mathrm{d}\,^{n+1}\lambda \end{pmatrix} = \begin{pmatrix} \mathbf{E}\,\mathrm{d}\,^{n+1}\boldsymbol{\epsilon} \\ \mathbf{0} \\ \mathbf{0} \end{pmatrix} \tag{7}$$

where $\mathbf{J}$ is the Jacobian of the local problem defined in equation (6). The upper-left block-matrix of the inverse of $\mathbf{J}$ contains the consistent tangent moduli. In the literature, compact expressions (after inverting $\mathbf{J}$ and taking the upper-left block-matrix) of these moduli can be found for particular models [3,15,23]. However, the more general expression given in equation (7) is preferred here because it highlights an important fact in the context of this work: the derivatives of the generalized flow vector needed to solve the local problem are also required in the computation of the consistent tangent matrix.

In Reference [14], numerical differentiation is used to approximate *directly* the consistent tangent moduli $\mathrm{d}^{n+1}\boldsymbol{\sigma}/\mathrm{d}^{n+1}\boldsymbol{\epsilon}$ (or, more precisely, an equivalent expression for the large-strain problems treated there). The resulting algorithm has a considerable CPU overhead in comparison to analytical derivation (40% to 80%) because the derivatives of *all* the stress components with respect to *all* the strain components are approximated numerically.

5

3 NUMERICAL DIFFERENTIATION

The derivatives of the generalized flow vector with respect to the generalized stresses are approximated by means of classical difference schemes. The approximation will be used for both the local and the global problems defined in the previous section. Thus, it must be accurate enough to maintain the characteristic quadratic convergence of the Newton-Raphson method.

Some authors [9,10] suggest to approximate numerically the second derivatives of the flow potential G (recall that the flow vector is the derivative of the flow potential). The standard approach to obtain second order of accuracy is the typical centered difference scheme [5,7,8] applied to a general n-dimensional function, $f(\mathbf{x})$:

$$\frac{\partial^2 f}{\partial x_i^2} = \frac{f(\mathbf{x} + h_i \mathbf{e}_i) - 2f(\mathbf{x}) + f(\mathbf{x} - h_i \mathbf{e}_i)}{h_i^2} + \mathcal{O}(h_i^2) \ . \tag{8}$$

In equation (8), x_i is the ith component of $\mathbf{x}$, $\mathbf{e}_i$ the ith unit vector, h_i the stepsize in the ith direction and the $\mathcal{O}$ denotes the order of convergence. The scheme represented by equation (8) will be denoted by 2ND-O(h^2), see table 1.

Notation	Description
1ND-O(h)	Forward difference scheme for first derivatives of the flow vector
1ND-O(h^2)	Centered difference scheme for first derivatives of the flow vector
1CND-O(h^2)	Approximation to first derivatives of the flow vector using complex variable
2ND-O(h^2)	Centered difference scheme for second derivatives of the flow potential

Table 1
Numerical approximations to the derivatives of the flow vector.

The approach used in this paper consists on approximating numerically the first derivatives of (the analytical expression of) the flow vector. That is, the flow vector can be obtained via analytical differentiation of the flow potential (this step is relatively simple, even for complex constitutive laws) or it can be an input of the model. Then, numerical differentiation is applied to approximate the derivatives of the flow vector (which is the computationally involved step for complex models). Standard forward or centered difference schemes are used:

$$\frac{\partial f}{\partial x_i} = \frac{f(\mathbf{x} + h_i \mathbf{e}_i) - f(\mathbf{x})}{h_i} + \mathcal{O}(h_i) \tag{9}$$

$$\frac{\partial f}{\partial x_i} = \frac{f(\mathbf{x} + h_i \mathbf{e}_i) - f(\mathbf{x} - h_i \mathbf{e}_i)}{2h_i} + \mathcal{O}(h_i^2) \ . \tag{10}$$

The schemes represented by equations (9) and (10) will be denoted by 1ND-O(h) and 1ND-O(h^2) respectively, see table 1.

It must be noted that the generic function f plays the role of a component of the flow vector in equations (9) and (10), whereas it denotes the flow potential in equation (8).

3.1 Error analysis

The key issue in numerical differentiation is the choice of the stepsize h_i. Approximations based on difference schemes are affected by truncation and rounding errors [5,28]. The truncation errors (represented in equations (8–10) with the $\mathcal{O}$ symbol) decrease as the stepsize tends to zero. The rounding errors, on the contrary, increase as the stepsize tends to zero. Therefore, there is an *optimal* stepsize h^{opt} that minimizes the summation of both errors.

Dennis and Schnabel [5] present an expression of this optimal stepsize for first and second-order approximations to first derivatives (1ND-O(h) and 1ND-O(h^2)) and for first-order approximation to second derivatives (not used in this paper). Their work has been extended here to the case of second-order approximation to second derivatives (2ND-O(h^2)).

The optimal stepsize h^{opt} can be written as

$$h^{\mathrm{opt}} = h_r^{\mathrm{opt}} \max\{|x|, \mathrm{typ}_x\}, \tag{11}$$

where h_r^{opt} is the optimal *relative* stepsize and typ_x is a typical value of x used to avoid choosing a null (or extremely small) h^{opt} for null (or extremely small) x. Numerical experimentation shows that typ_x can be chosen in a rather arbitrary manner, because it has a very small influence on the results (in all the numerical examples of section 4, $\mathrm{typ}_x = 1$). The main idea behind equation (11) is that h_r^{opt} is independent of x. This means that a constant value of h_r^{opt} can be used all over the domain, for every load step, and all the stress components.

In general, it is not possible to compute the exact value of h_r^{opt}. This would require the rigorous minimization of the sum of truncation and rounding errors. However, the following expressions can be found after some simplifying assumptions:

7

$$1\text{ND} - \text{O}(h) : h_r^{\text{opt}} = \sqrt{\eta} \tag{12}$$

$$1\text{ND} - \text{O}(h^2) : h_r^{\text{opt}} = \sqrt[3]{\eta} \tag{13}$$

$$2\text{ND} - \text{O}(h^2) : h_r^{\text{opt}} = \sqrt[4]{\eta} \tag{14}$$

In equations (12–14), η is the accuracy in the evaluation of f. The expressions (12) and (13) are given by Dennis and Schnabel [5]. Expression (14) has been derived following the same arguments, as described next.

Consider equation (8). A standard error propagation analysis renders the following bound on the rounding error E^{Ro} in the approximation to the second derivative, i.e. errors induced by finite precision computations of the first term in the RHS of equation (8):

$$|\text{E}^{\text{Ro}}| \leq \frac{(4\eta + 12r)\hat{f}}{h^2} . \tag{15}$$

In equation (15), r is the machine precision ($r \approx 10^{-16}$ in IEEE double precision), $\hat{f}$ is an upper bound of $|f|$ in the neighborhood of x and the subscript i is ommited from the stepsize h to ease the notation.

Regarding the truncation error E^{Tr}, i.e. the second term in the RHS of equation (8), a bound can be easily derived [7,8] as

$$|\text{E}^{\text{Tr}}| \leq \frac{\gamma h^2}{12} , \tag{16}$$

where γ is a bound on the fourth derivative of f. Putting equations (15) and (16) together, the following bound on the total error E^{Tot} is obtained:

$$|\text{E}^{\text{Tot}}| \leq |\text{E}^{\text{Tr}}| + |\text{E}^{\text{Ro}}| \leq \frac{\gamma h^2}{12} + \frac{(4\eta + 12r)\hat{f}}{h^2} . \tag{17}$$

The effect of the truncation error and the rounding error on the total error is clearly highlighted in a double logarithmic graph of E^{Tot} versus h: the rounding error contributes with a line of slope 2 (because second derivatives are approximated) and the truncation error with a line of slope -2 (because a second-order scheme is used). Similar results are obtained for the other schemes, see [5] and figures 1 and 3 of subsection 4.1.

The optimal value of the stepsize, which minimizes the bound of $|\text{E}^{\text{Tot}}|$ given by equation (17) is

$$h^{\text{opt}} = \sqrt[4]{12(4\eta + 12r)\frac{\hat{f}}{\gamma}} . \tag{18}$$

The value of h^{opt} cannot be computed from equation (18): the values of $\hat{f}$ and γ depend on x, and, in general, they are very difficult to approximate.

8

Following Dennis and Schnabel [5], it is assumed that

$$\frac{\hat{f}}{\gamma} \propto (\max\{|x|, \mathrm{typ}_x\})^4 \,, \tag{19}$$

where the fourth power is obtained as the sum of the degree of derivation and the order of the approximation (2 and 2), and $\propto$ means "is proportional to". This assumption is rather reasonable; it is verified, for instance, for monomials $f(x) = x^\alpha$. Combining equations (18) and (19) yields

$$h^{\mathrm{opt}} \propto \sqrt[4]{\max\{\eta, r\}} \max\{|x|, \mathrm{typ}_x\} \,. \tag{20}$$

Two further assumptions are needed: 1) η is larger or equal to r (if function f is simple, then η is similar to r, but if many operations are involved, η can be quite larger than r) and 2) the proportionality constant can be taken as 1 (again a reasonable assumption, as illustrated by monomials $f(x) = x^\alpha$). With these assumptions, one finally gets the expression of the relative optimal stepsize given in equation (14).

The concept of *relative* stepsize is essential in computational plasticity. In a global problem the range of values of the generalized stresses is usually very large, and the values of the different components at a certain Gauss point are very different. For this reason, the optimal stepsize h^{opt} can show huge variations. However, the previous analysis shows that the optimal relative stepsize h_r^{opt} can be assumed to be constant. Since a simple technique is wanted, the same value of h_r^{opt} (obtained from equations (12), (13) or (14), depending on the scheme) will be used for all the computation. In fact, equations (12–14) are only used to select the *order of magnitude* of h_r^{opt}, because there is a wide range of relative stepsizes for which the difference schemes (8–10) are accurate enough to attain quadratic convergence. In this context, the assumptions needed to deduce the simplified expressions of h_r^{opt}, equations (12–14), do not restrict at all the applicability of the proposed approach. This point is illustrated in the next section by means of several numerical examples.

Remark 1 *An unconventional approximation of first derivatives has also been used in this work. It is based on the theory of functions of complex variable [12,27]. If $f : \mathbb{C} \to \mathbb{C}$ is analytic in a neighborhood that contains the point $z = (x, 0)$ (with $z \in \mathbb{C}$ and $x \in \mathbb{R}$) the first derivative of $f : \mathbb{R} \to \mathbb{R}$ at x can be approximated with second order of accuracy as*

$$\frac{\mathrm{d}f}{\mathrm{d}x} = \frac{\mathrm{Im}(f(x + ih))}{h} + \mathcal{O}(h^2) \tag{21}$$

where $i = \sqrt{-1}$ and $\mathrm{Im}(f)$ represents the imaginary part of f. The main feature of this approximation is that it involves no subtractions, so the cancellation error typical of finite difference schemes (see equations (9) and (10)) is

avoided. The scheme represented by equation (21) will be denoted by 1CND-O(h^2), *see table 1. In many applications, but not in all, this approach has the advantage that it is not necessary to choose a stepsize close to the optimal one. In the next section, this approach is applied to some examples of computational plasticity, and the main issues are discussed. Further applications will be presented in a forthcoming paper [17].*

4   EXAMPLES

In this section, the applicability of numerical differentiation to solve the local and the global problem is assessed. Two plasticity models are used: the Von Mises model, with perfect plasticity and with exponential hardening [3,25], and the Rounded Hyperbolic Mohr-Coulomb (RHMC) model [1,26]. The Von Mises flow potential depends only on the second invariant of the stress tensor, thus the analytical derivatives of the flow vector are simple to compute. It is used just as a validation test. The RHMC flow potential depends on the three invariants through a complicated expression. The analytical derivatives of the flow vector have quite involved expressions. Thus, it is a good model to check the performance of numerical differentiation.

In subsection 4.1, the analytical derivatives of the flow vector are compared with the numerical approximations. Four possibilities for the evaluation of the numerical derivatives are analyzed (see table 1). The values of the optimal relative stepsize and the influence of the rounding and truncation errors are presented. In subsection 4.2, the numerical differentiation is applied to the computation of the Jacobian of the residual of the local problem. An example with the RHMC model is presented. It will be shown that any of the four numerical approximations defined in table 1 can be used to solve the local problem.

Finally, in subsection 4.3, the numerical differentiation is applied to the computation of the consistent tangent matrix (global problem). Four examples are presented, two with Von Mises plasticity and two with the RHMC model.With Von Mises plasticity, a perforated strip under traction is analyzed [25], first considering perfect plasticity and after with exponential hardening. With the RHMC model, the vertical displacement of a pile [18] and the behavior of a rigid footing [1] are simulated. It will be shown that approximating numerically the first derivatives of the flow vector maintains the quadratic convergence of the Newton-Raphson method for a wide range of relative stepsizes, and that approximating the second derivatives of the flow potential does not.

4.1 Comparison of numerical differentiation with analytical derivatives

In the following, analytical derivatives are compared with four numerical approximations: difference schemes of first and second-order of accuracy for first derivatives of the flow vector, 1ND-O(h) and 1ND-O(h^2) respectively; a difference scheme of second-order of accuracy for second derivatives of the flow potential, 2ND-O(h^2); and the approximation to the first derivatives of the flow vector based on complex variable theory defined in equation (21), 1CND-O(h^2). The four approximations are summarized in table 1.

In this subsection, analytical derivatives are compared with the four numerical approximations summarized in table 1. The influence of the relative stepsize on the rounding, truncation and total errors is analyzed. In subsections 4.2 and 4.3 the numerical differentiation will be applied to the local and the global problems respectively.

4.1.1 Von Mises model

The first example deals with the derivatives of the Von Mises flow vector. The difference schemes present the typical relationship between the relative error of the approximation versus the relative stepsize (see figure 1). The influence of the different errors is clear: the left part of the curves correspond to the rounding errors and the right part to the truncation errors. Each of them have the expected slope. Moreover, the optimal relative stepsize h_r^{opt} of each approximation is in agreement with the corresponding expression, equations (12), (13) and (14), with $\eta \approx 10^{-16}$. The value of η is close to r because the computation of the flow vector is very simple. In figure 1 the relative error of the 1CND-O(h^2) approximation is also depicted. The main advantage of this approximation is that rounding errors are typically constant (i.e., they do not increase as the stepsize tends to zero) and very small. Thus, an arbitrarily small stepsize may be used. In subsection 4.3 this approach will be applied to the global problem and the main advantages will be highlighted.

The curves of figure 1 have been computed with a stress state where all the stress components are of the same order of magnitude. If this situation is maintained, the level of stress does not affect figure 1: the same curves are obtained for any level of stress. However, in a typical global problem the various components of the stress tensor can be very different (up to four orders of magnitude). It has been verified experimentally that, in these cases, the curves depicted in figure 1 are shifted to the right (the value of the h_r^{opt} can grow up to three orders of magnitude). For the numerical approximations to first derivatives of the flow vector (1ND-O(h), 1ND-O(h^2) and 1CND-O(h^2)), this situation does not represent any practical problem. It will be shown in
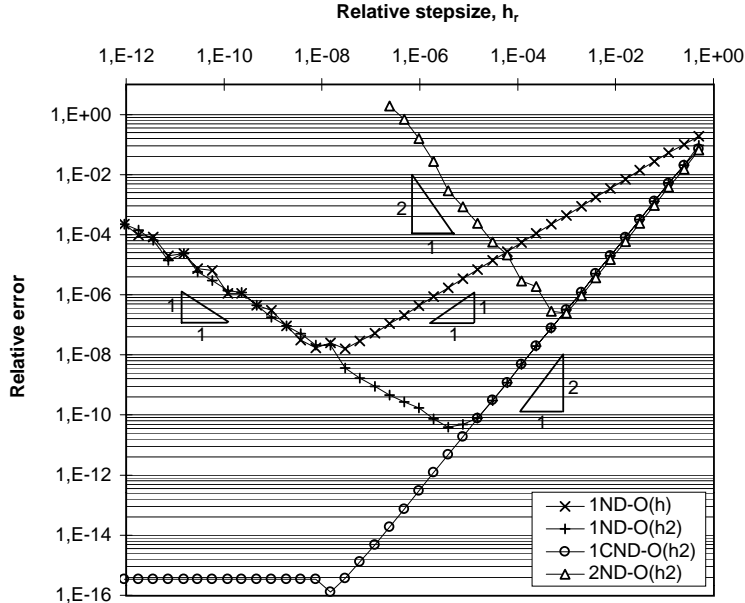
11

Figure 1. Relation between the relative error of the numerical approximations to the flow vector derivatives versus the relative stepsize, Von Mises model.

subsections 4.2 and 4.3 that the range of relative stepsizes that give good results is large enough. Nevertheless, for the numerical approximation to second derivatives of the flow potential (2ND-O(h^2)), the curve is also shifted upwards: the value of the minimum relative error (i.e., the relative error at h_r^{opt}) can grow up to three orders of magnitude. Therefore, it can be anticipated that approximating the second derivatives of the flow potential is less adequate than approximating the first derivatives of the flow vector.

4.1.2 Rounded Hyperbolic Mohr-Coulomb model

The numerical approximations to the flow vector derivatives of the Rounded Hyperbolic Mohr-Coulomb (RHMC) model have been also analyzed. The definition of the flow potential and its derivatives is presented by Abbo [1]. The main features of the flow potential are summarized in figure 2 (associated plasticity is considered, so the yield function and the flow potential coincide). The definition of the flow potential is divided into two regions: one corresponding to the Hyperbolic Mohr-Coulomb zone that smoothes the apex of the classical Mohr-Coulomb model on the hydrostatic axis, and the other corresponding to the rounding zones, that smooth the corners present on the deviatoric plane.

The relation between the relative error and the relative stepsize for the four numerical approximations (summarized in table 1) is depicted in figure 3. Results are very similar to those obtained with Von Mises plasticity (figure 1). The main difference between the two models is the behavior of the 1CND-

12
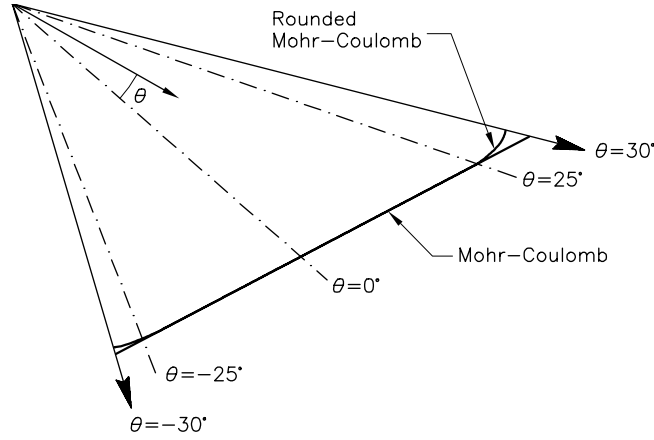
(a)
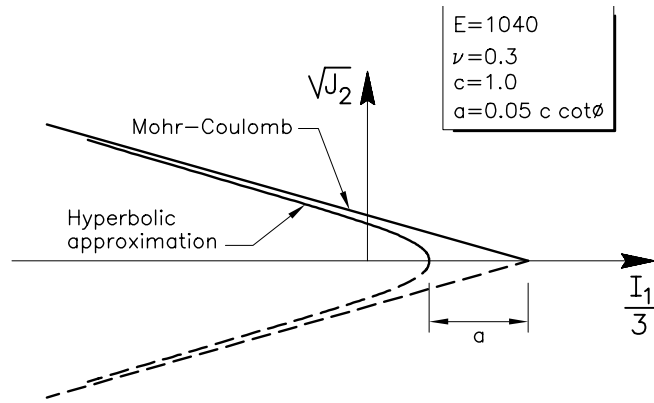
(b)

Figure 2. Main features of the Rounded Hyperbolic Mohr-Coulomb yield surface: (a) deviatoric plane, (b) invariant space (after Abbo [1]).

$O(h^2)$ approximation. For the RHMC model, this approximation presents the same features of 1ND-$O(h^2)$, the standard second-order approximation to the first derivative: rounding errors are not constant. This is caused by the routine used for the evaluation of the arcsin function (which appears in the RHMC model, see [1]) of a complex argument. FORTRAN compilers typically do not include the arcsin of a complex argument as an intrinsic function. For this reason, a transformation based on logarithms was used for the computations shown here. This transformation is the origin of the non-constant rounding errors. If the arcsin is computed in a more accurate way (like the algebraic manipulator Maple does, for instance), constant and very small rounding errors are obtained, and the 1CND-$O(h^2)$ approximation exhibits its general behavior, illustrated in figure 1. However, with the routine used here rounding errors are not constant, so there is no improvement in using complex variables. In consequence, the approximation 1CND-$O(h^2)$ will not be used in the examples with the RHMC model of subsections 4.2 (local problem) and 4.3 (global problem).
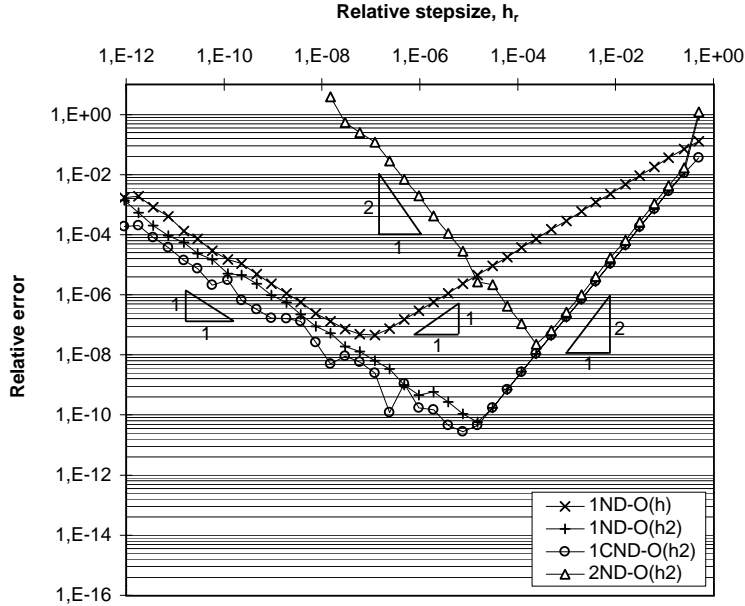
Figure 3. Relation between the relative error of the numerical approximations to the flow vector derivatives versus the relative stepsize, RHMC model.

4.2 Application to the local problem

Numerical differentiation is applied in order to compute the Jacobian shown in equation (6). Only the RHMC model is considered. Examples with Von Mises model are not presented because with perfect plasticity the local problem is linear, and with exponential hardening the (nonlinear) local problem is so simple that the numerical approximations perform almost identically to the analytical derivatives.

In the local problem of the RHMC model, the Newton-Raphson method with the standard elastic predictor (the trial stresses, without any additional improvement) presents regions of non-convergence in the stress space [1]. However, in large regions of the stress space the local problem converges in few iterations, due to the special linear form of the yield surface. In order to check the applicability of numerical differentiation, a trial stress point located in an intermediate position has been chosen.

Figure 4 shows the convergence results of the local problem obtained with analytical derivatives and with the numerical approximations 1ND-O(h), 1ND-O(h^2) and 2ND-O(h^2) (the 1CND-O(h^2) approximation is not used with the RHMC model because it presents the same behavior that 1ND-O(h^2), see figure 3). It is a plane strain problem, and the values of the material parameters are in figure 2. The trial stresses are $\sigma_{xx} = -15$, $\sigma_{yy} = -10$, $\sigma_{zz} = -5$ and $\sigma_{xy} = 15$. The converged stresses are $\sigma_{xx} = -20.5$, $\sigma_{yy} = -17.2$, $\sigma_{zz} = -10.2$

14

1ND - O(h)

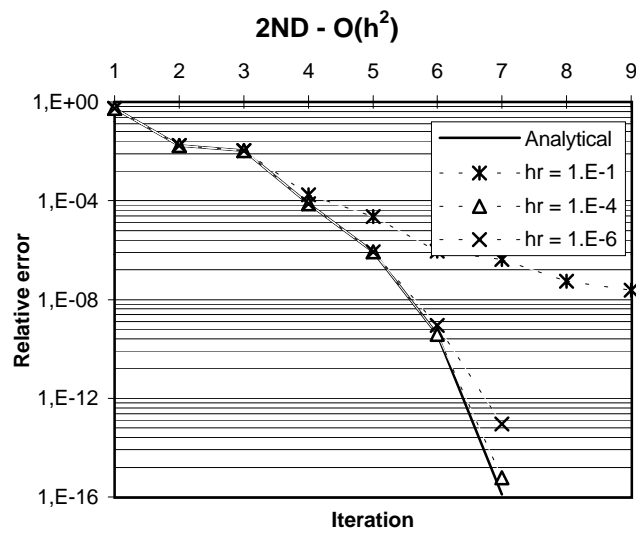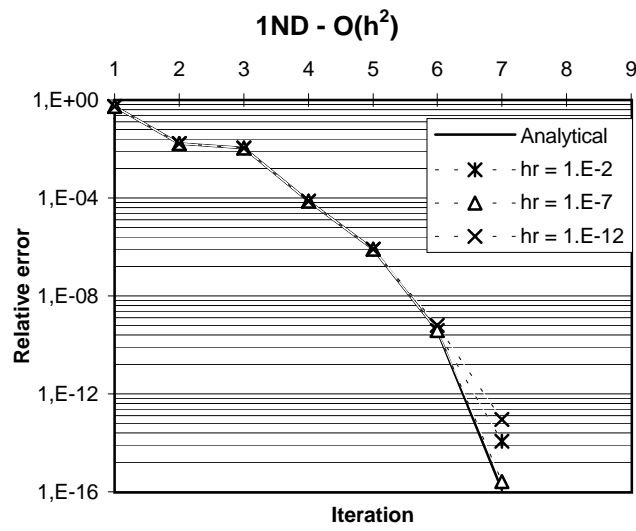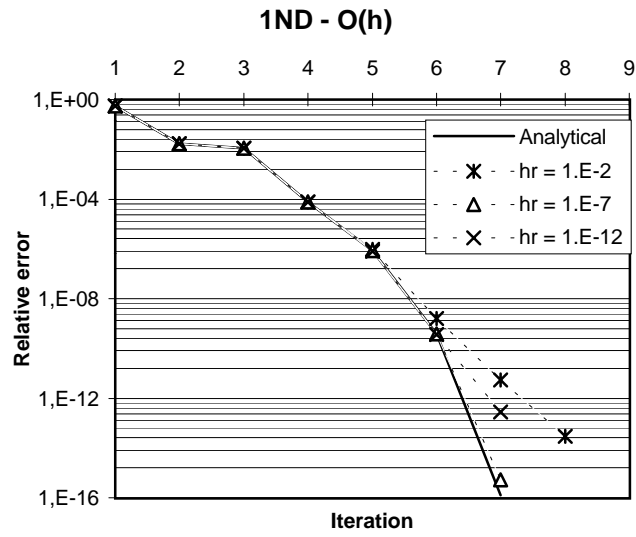

1ND - O(h^2)

2ND - O(h^2)

Figure 4. Convergence results of the local problem with RHMC model.

and $\sigma_{xy} = 9.98$. The problem is highly nonlinear: the Lode angle (defined in figure 2) changes from 16° at the trial state (Hyperbolic Mohr-Coulomb zone) to 26.5° at the converged state (Rounded zone).

The results of figure 4 show that, for the approximations 1ND-O(h) and 1ND-O(h^2), quadratic convergence is achieved for a wide range of stepsizes. It is only lost if the relative stepsize is very different from the optimal one. On the contrary, the 2ND-O(h^2) approximation is quite more sensible to the value of h_r. Numerical experimentation reveals that the key point for quadratic convergence is to use a h_r such that the relative error of the corresponding approximation of the analytical derivatives is less than $10^{-5} - 10^{-6}$. It can be checked in figure 3 that this constraint yields a large interval of acceptable relative stepsizes for the numerical approximations to first derivatives of the flow vector, and a quite narrower one for the numerical approximation to second derivatives of the flow potential. In any case, the three difference schemes (1ND-O(h), 1ND-O(h^2) and 2ND-O(h^2)) are valid for the local problem.

4.3   Application to the global problem

Numerical differentiation is applied to solve several boundary value problems (i.e., global problems). That is, the numerical approximations of table 1 are employed to compute consistent tangent matrices. Moreover, in the examples with the RHMC model, they are also used to solve the local problem. For all the stress components and over the whole domain a constant relative stepsize has been used.

Four examples are presented: two with Von Mises plasticity and two more with the RHMC model. These examples will illustrate that any numerical approximation to first derivatives of the flow vector (1ND-O(h), 1ND-O(h^2) and 1CND-O(h^2)) is useful to solve the global problem with quadratic convergence. On the contrary, approximating numerically the second derivatives of the flow potential (2ND-O(h^2)) is not robust enough to achieve quadratic convergence.

4.3.1   Von Mises model with perfect plasticity

First, a perforated strip under uniaxial traction is analyzed with Von Mises perfect plasticity. This test is presented by Simo and Taylor [25], and it is depicted in figure 5. A total displacement of 0.2 m is imposed in ten steps.

The convergence results for the fourth and the eighth load steps obtained with the analytical consistent tangent matrix and with numerical differentiation are compared in figure 6. The ranges of relative stepsizes that give the
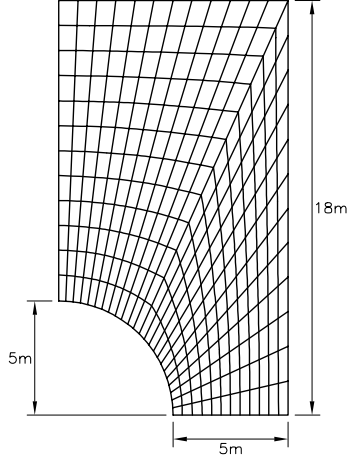
16

Figure 5. Perforated strip under traction (after Simo [25]). Due to symmetry, only one quarter is considered.

same convergence results that analytical consistent tangent matrix (up to a relative error in energy of 10^{-12}) are presented in table 2 (convergence results are considered to be the *same* if the energy error has the same order of magnitude during all the iterations of all the load steps). Also in table 2, between parenthesis, the values of h_r that give *almost the same* results as the analytical derivatives are indicated (convergence results are considered to be *almost the same* if the energy error has the same order of magnitude during all the iterations except the last one of each load step). It can be seen that the difference schemes for first derivatives, 1ND-O(h) and 1ND-O(h^2), give the same result that analytical differentiation for a wide range of relative stepsizes, even though a very strict tolerance has been used. As expected, second-order of accuracy presents a wider range of adequate relative stepsizes than first-order. The 1CND-O(h^2) approximation presents the same convergence results as the 1ND-O(h^2) one for relative stepsizes higher than the optimal one. Moreover, in agreement with the results of subsection 4.1 (see figure 1), it maintains the quadratic convergence for arbitrarily small relative stepsizes. On the other hand, the numerical difference scheme for second derivatives of the flow potential, 2ND-O(h^2), does not give very good results even in this simple boundary value problem (the typical quadratic convergence is lost).

Num. approx.	Range of h_r
1ND-O(h)	$(10^{-4}) - 10^{-5} - 10^{-7} - (10^{-8})$
1ND-O(h^2)	$(10^{-2}) - 10^{-3} - 10^{-8} - (10^{-9})$
1CND-O(h^2)	$(10^{-2}) - 10^{-3} - \ldots$
2ND-O(h^2)	(10^{-2})

Table 2
Relative stepsizes that give the same convergence results as analytical derivatives, for the Von Mises perfect plasticity global problem.
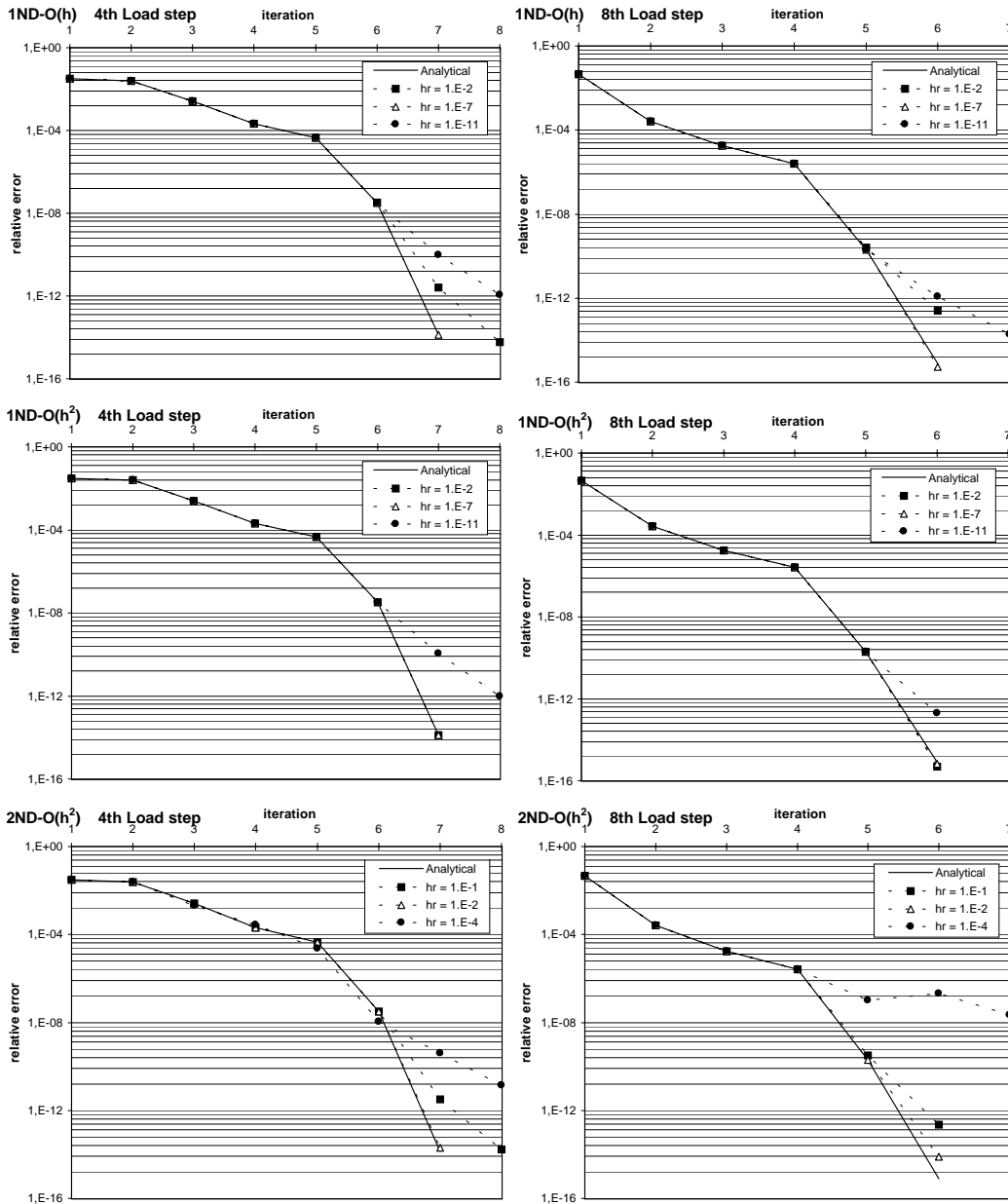
Figure 6. Convergence results for the fourth and the eighth load steps. Von Mises perfect plasticity.

4.3.2 Von Mises model with exponential isotropic hardening

The perforated strip under traction has also been simulated using the Von Mises model with exponential isotropic hardening. The problem definition is the same of Reference [25], except for the plastic parameters: the initial yield stress is equal to 0.243 MPa, the yield stress at infinite equivalent plastic strain is 0.729 MPa and the exponential parameter is 0.1 MPa. In figure 7, the convergence results for the fourth and the eighth load steps are depicted, and in table 3 the ranges of relative stepsizes that give the same convergence
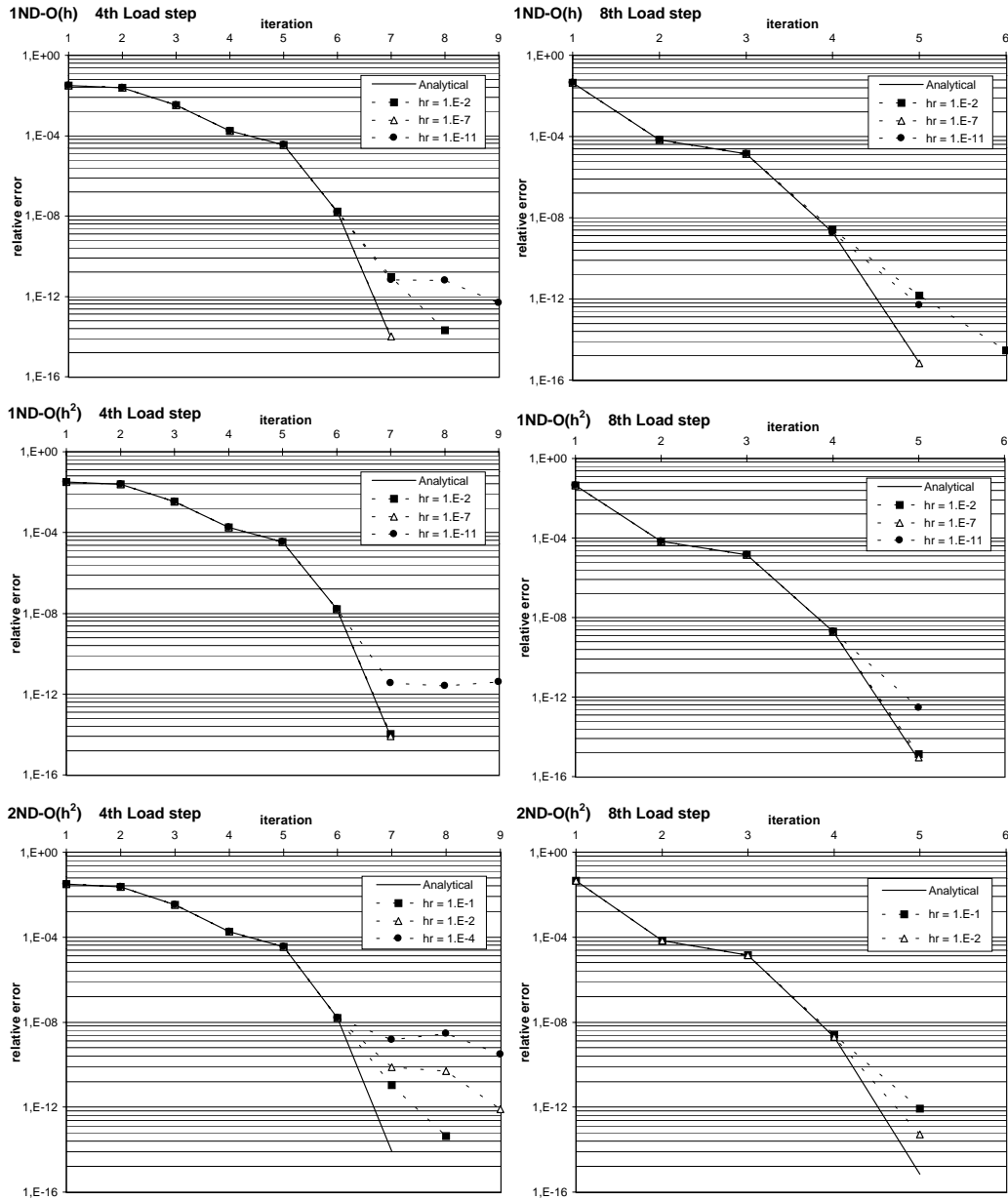
Figure 7. Convergence results for the fourth and the eighth load steps. Von Mises exponential hardening plasticity.

Num. approx.	Range of h_r
1ND-O(h)	$(10^{-4}) - 10^{-5} - (10^{-6})$
1ND-O(h^2)	$10^{-3} - 10^{-5} - (10^{-6}) - (10^{-7})$
1CND-O(h^2)	$10^{-3} - \ldots$
2ND-O(h^2)	$-$

Table 3
Relative stepsizes that give the same convergence results as analytical derivatives, for the Von Mises exponential hardening global problem.

results that analytical consistent tangent matrices are presented. The results are more strict than those obtained with perfect plasticity: numerical first derivatives present a narrower range of relative stepsizes that give the same results as analytical derivatives, and the numerical second derivatives do not attain quadratic convergence. Moreover, note that the optimal relative stepsize is higher than the one of figure 1. This is in agreement with the previous comments about the value of h_r^{opt} when the components of the stress tensor have very different values. On the other hand, the 1CND-O(h^2) approximation presents the same behavior as in perfect plasticity: the results are the same as the 1ND-O(h^2) approximation for h_r higher than the optimal one, and quadratic convergence is achieved for arbitrarily small h_r.

The main conclusion of the two examples with Von Mises plasticity is that numerical first derivatives of the flow vector do not affect the properties of convergence of the Newton-Raphson method (i.e., the global consistent tangent matrix is accurately approximated). The typical difference schemes present an adequate behavior for a wide range of relative stepsizes. And the unconventional approximation based on complex variable theory allows to use stepsizes as small as wanted. On the other hand, it has been shown that the numerical second derivatives of flow potential are not robust enough: they do not work properly in demanding boundary value problems.

In the following, the applicability of the approximations 1ND-O(h), 1ND-O(h^2) and 2ND-O(h^2) to the Rounded Hyperbolic Mohr-Coulomb (RHMC) model is assessed by means of two boundary value problems. In both problems numerical differentiation is applied to the local and the global problem simultaneously.

4.3.3 RHMC model: vertical displacement of a pile

The first problem is the vertical displacement of a pile. The definition of the problem is presented by Potts and Gens [18], and it is only summarized here. Figure 8 shows the finite element mesh. It corresponds to a horizontal disc of soil. The thickness of the disc is 5 units of length (u.l.) and the pile radius is 7.5 u.l. To model the loading of the pile, a vertical displacement of 2 u.l. is imposed over the boundary AF in 20 load steps. To model the infinite extension of the
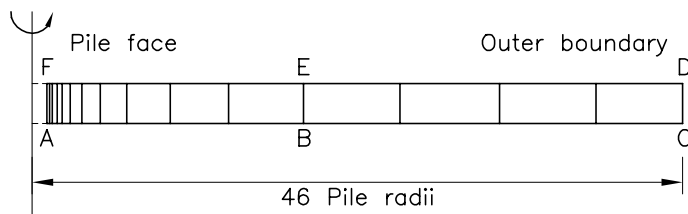

Figure 8. Pile problem (after Potts and Gens [18]).

20

a)	Analytic	10^{-3}	10^{-5}	10^{-7}	10^{-9}
1	2.2 E+00	2.2 E+00	2.2 E+00	2.2 E+00	2.2 E+00
2	1.5 E-03	1.5 E-03	1.5 E-03	1.5 E-03	1.5 E-03
3	3.1 E-05	3.1 E-05	3.1 E-05	3.1 E-05	3.1 E-05
4	8.6 E-09	1.3 E-07	8.6 E-09	8.6 E-09	8.6 E-09
5	4.6 E-15	1.7 E-09	4.7 E-15	1.4 E-13	8.0 E-12
6		2.6 E-11			8.7 E-12
7		3.4 E-13			1.1 E-11
8					. . .

b)	Analytic	10^{-2}	10^{-3}
1	2.2 E+00	2.2 E+00	2.2 E+00
2	1.5 E-03	1.5 E-03	1.5 E-03
3	3.1 E-05	4.0 E-05	3.0 E-05
4	8.6 E-09	7.2 E-06	1.8 E-07
5	4.6 E-15	8.6 E-07	1.7 E-08
6		1.3 E-07	1.5 E-09
7		1.7 E-08	1.4 E-10
8		2.4 E-09	1.3 E-11
9		3.2 E-10	1.2 E-12
10		4.5 E-11	2.1 E-13
11		. . .	

Table 4
The convergence results for sixth load step of the pile problem: a) 1ND-O(h), b) 2ND-O(h^2).

Num. approx.	Range of h_r
1ND-O(h)	$(10^{-4}) - 10^{-5} - (10^{-6})$
1ND-O(h^2)	$10^{-4} - 10^{-6} - (10^{-7})$
2ND-O(h^2)	$-$

Table 5
Relative stepsizes that give the same convergence results as analytical derivatives, for the pile problem.

disc, zero vertical displacement is imposed over the boundary CD. Due to the essentially one-dimensional nature of the problem, vertical lines (such as EB) are prescribed to remain vertical during loading.

Table 4 shows the convergence results for the tenth load step, and in table 5 the ranges of relative stepsizes that give the same convergence results that analytical consistent tangent matrices are presented. It is clear that the numerical approximations to the second derivatives of the flow potential, 2ND-O(h^2), do not yield quadratic convergence. To reach quadratic convergence it would be

necessary to do a supplementary effort to choose a correct stepsize at each Gauss point. The results of the approximation 1ND-O(h) are quite similar to the previous example, see table 3. The h_r that gives quadratic convergence in the global problem is higher than the estimated value from an analysis of the approximations to the flow vector derivatives (see figure 3). This is in agreement with the previous analysis of the influence of the stresses on the value h_r^{opt}. On the other hand, although one may conclude from table 5 that the range of adequate h_r is quite small, it must be pointed out that the comparison has been done up to a very strict tolerance of 10^{-12}. If the results are compared to a tolerance of 10^{-8} (that for a relative energy error is still a strict tolerance), the range becomes 10^{-4} to 10^{-9}. Thus, the 1ND-O(h) approximation is accurate enough.

The results of 1ND-O(h^2) are also similar to previous ones: the range of adequate h_r is larger than for 1ND-O(h), see table 5. Nevertheless, if realistic tolerances are considered (i.e., 10^{-8} or higher), the advantage of second order approximation is lost: the two alternatives give good results for a very wide range of relative stepsizes. Moreover, since the computational cost (the number of evaluations of the flow vector) of the first-order approximation is half of the second-order one, it can be concluded that the first-order scheme is more suitable.

4.3.4   RHMC model: vertical displacement of a rigid footing

The second global problem solved using the RHMC model is the vertical displacement of a rigid footing [1]. The scheme of the problem is depicted in figure 9a, and the mesh and the final distribution of plastic strains are shown in figure 9b. The dimension of the rigid footing, B, is 20 units of length (u.l.) and a vertical displacement of 0.02 u.l. is imposed in 20 increments.

The convergence results for the load steps fifteen and twenty are shown in figure 10, and the ranges of relative stepsizes that give the same convergence results that analytical consistent tangent matrices are presented in table 6. The results are similar to previous ones: the 1ND-O(h) approximation gives quadratic convergence with a small range of relative stepsizes if a very strict tolerance is used (10^{-12}), and with second-order of accuracy, 1ND-O(h^2), the range of relative stepsizes is wider. However, as in the pile problem example, with a tolerance of 10^{-8} almost any relative stepsize gives good results for both approximations. Therefore, for practical applications the first-order difference scheme approximation, 1ND-O(h), is accurate enough. Moreover, the choice of the relative stepsize is not a problem (as in the previous example, the values of h_r between 10^{-4} and 10^{-9} give quadratic convergence up to a relative error less than 10^{-8}).
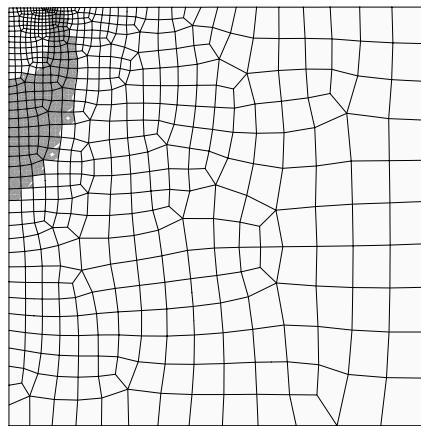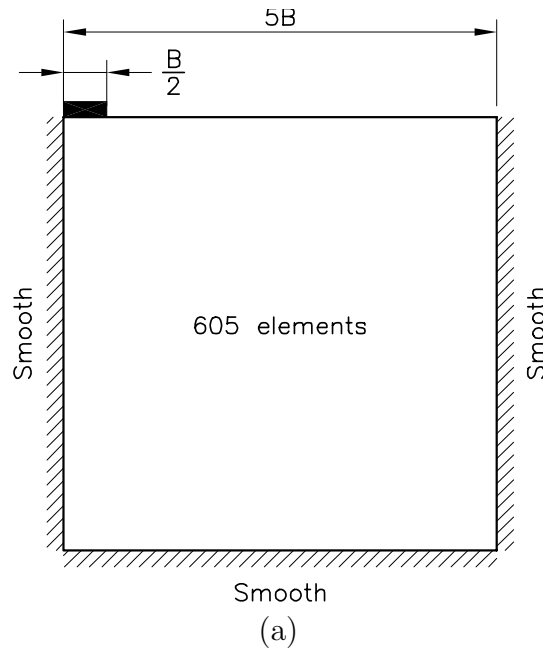
(a)

(b)

Figure 9. Rigid footing: (a) problem definition, (b) mesh and final plastic strains. Due to symmetry, only one half is considered.

In this global problem, the computing time of the alternatives 1ND-O(h) and 1ND-O(h^2) has been analyzed. In table 7 there are the time overheads with respect to the problems solved with analytical consistent tangent matrices. All the approximations, except 1ND-O(h) with $h_r = 10^{-3}$, have needed the same number of iterations. For this particular case, the 1ND-O(h) approximation is between 1–1.5% more expensive than the one computed with the analytical derivatives, and the 1ND-O(h^2) is between 2.6–2.8%. Therefore, the computational cost of the proposed approach is marginal, even in the context of material models (Von Mises and RHMC) where analytical derivatives are available and relatively simple to compute.
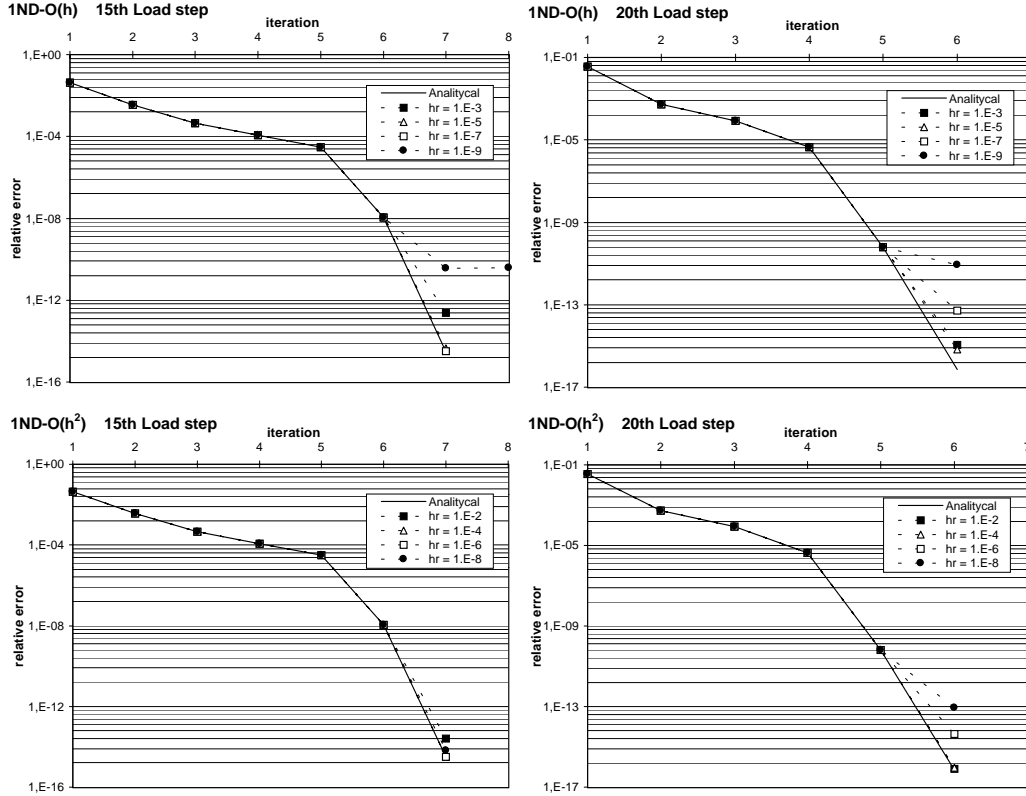
Figure 10. Convergence results for the load steps fifteen and twenty. Rigid footing with RHMC model.

The main conclusion of these last two examples is that typical difference schemes applied to first derivatives of the flow vector are adequate to approximate the consistent tangent matrix and the Jacobian of the residual of the integration rule for highly nonlinear flow potentials. The convergence properties are the same that with analytical derivatives for a wide range of relative stepsizes. The first-order approximation is enough to maintain quadratic convergence up to a tolerance of less than 10^{-8}. Nevertheless, for tolerances less or equal to 10^{-12}, second-order accuracy is needed in order to have a wide range of relative stepsizes. Finally, for complex models the numerical second derivatives of the flow potential are not robust enough to maintain quadratic convergence, even in simple boundary value problems.

Num. approx.	Range of h_r
1ND-O(h)	$(10^{-4}) - 10^{-5} - (10^{-6}) - (10^{-7})$
1ND-O(h^2)	$(10^{-2}) - 10^{-3} - 10^{-5} - (10^{-6}) - (10^{-8})$

Table 6
Relative stepsizes that give the same convergence results as analytical derivatives, for the rigid footing problem.

24

h_r	1ND-O(h)	1ND-O(h^2)
10^{-3}	4.1%	2.8%
10^{-4}	2.5%	3.4%
10^{-5}	1.5%	2.6%
10^{-6}	1.0%	2.8%
10^{-7}	1.4%	2.6%
10^{-8}	1.2%	3.8%

Table 7
Time overheads of the numerical approximations, for the rigid footing problem.

5 CONCLUSIONS

It has been shown that numerical differentiation is a useful tool in computational plasticity, both in the integration of the constitutive law (local problem) and in the computation of the consistent tangent matrix (global problem).

The analytical derivatives of the generalized flow vector with respect to the generalized stresses are the components most difficult to compute in the consistent tangent matrix and the Jacobian of the local residual. In some cases, they are not even available. The main conclusion of this paper is that numerical differentiation is a valid alternative to analytical derivatives.

Two approaches are possible: 1) approximating the second derivatives of the flow potential (recall that the flow vector is the first derivative of the flow potential) or 2) approximating the first derivatives of the (analytical) flow vector. The first approach, suggested in the literature, is not robust enough. It can be used to solve the local problem, but not the global problem. The resulting consistent tangent matrices are not accurate enough and the Newton-Raphson method looses its characteristic quadratic convergence. The second approach, on the contrary, is a simple and robust alternative to analytical differentiation. Quadratic convergence is achieved, both for simple (Von Mises) and more complicated (Rounded Hyperbolic Mohr-Coulomb) material models.

Various schemes may be used to approximate the first derivatives of the flow vector: the classical first-order and second-order difference schemes, and an unconventional second-order approximation based on complex variable theory. The first-order approximation maintains quadratic convergence up to a tolerance of less than 10^{-8}, and the second-order approximations up to less than 10^{-12}. Thus, all of them are accurate enough for any practical application.

The choice of an adequate stepsize (a typical problem of difference schemes) does not present any difficulty. The concept of the relative stepsize has been presented, and it has been verified that the three approximations to first derivatives of the flow vector give good results with a wide range of relative

stepsizes. That is, the proposed strategy is very robust in the sense that the choice of the stepsize has a very small influence on its performance. Moreover, the complex variable approximation presents a very interesting property: the rounding errors are very small and constant (i.e., they do not increase as the stepsize tends to zero), so arbitrarily small stepsizes may be used.

The computational overhead of the proposed strategy (with repect to analytical derivatives) is marginal, even for material models where the analytical derivatives have relatively simple expressions. This result is in sharp contrast with previous applications of numerical differentiation to computational plasticity [9,10,14]. In a forthcoming paper [17], numerical differentiation will be applied to more complex constitutive models, where analytical derivatives are not available.

References

[1] A. J. Abbo. *Finite element algorithms for elastoplasticity and consolidation.* PhD thesis, University of Newcastle, Newcastle, February 1997.

[2] J. L. Chaboche and G. Cailletaud. Integration methods for complex plastic constitutive equations. *Computer Methods in Applied Mechanics and Engineering*, 133:125–155, 1996.

[3] M. A. Crisfield. *Non-linear finite element analysis of solids and structures. 1 Essentials.* John Wiley & Sons, Chichester, 1991.

[4] M. A. Crisfield. *Non-linear finite element analysis of solids and structures. 2 Advanced topics.* John Wiley & Sons, Chichester, 1997.

[5] J. E. Dennis and R. B. Schnabel. *Numerical methods for unconstrained optimization and nonlinear equations.* Prentice-Hall, New Jersey, 1983. (Reprinted by Siam, Classics in Applied Mathematics, 1996).

[6] G. Etse and K. Willam. Fracture energy formulation for inelastic behavior of plain concrete. *Journal of Engineering Mechanics*, 120(9):1983–2011, 1994.

[7] J. D. Hoffman. *Numerical methods for engineers and scientists.* Prentice-Hall, New Jersey, 1982.

[8] E. Isaacson and H. B. Keller. *Analysis of numerical methods.* Constable and Company, London, 1966. (Reprinted by Dover Publications, 1994).

[9] B. Jeremić and S. Sture. Implicit integrations rules in plasticity: Theory and implementation. Technical report, Report to NASA Marshall Space Flight Center, Contract: NAS8-38779, University of Colorado at Boulder, Jul. 1994.

[10] B. Jeremić and S. Sture. Implicit integrations in elastoplastic geotechnics. *Mechanics of Cohesive-Frictional Materials*, 2:165–183, 1997.

[11] J. Lubliner. *Plasticity theory*. Macmillan Publishing Company, New York, 1990.

[12] J. N. Lyness and C. B. Moler. Numerical differentiation of analytic functions. *SIAM Journal of Numerical Analysis*, 4:202–210, 1967.

[13] E. J. Macari, S. Weihe, and P. Arduino. Implicit integration of elastoplastic constitutive models for frictional materials with highly non-linear hardening functions. *Mechanics of Cohesive-Frictional Materials*, 2:1–29, 1997.

[14] C. Miehe. Numerical computation of algorithmic (consistent) tangent moduli in large-strain computational inelasticity. *Computer Methods in Applied Mechanics and Engineering*, 134:223–240, 1996.

[15] M. Ortiz and J. B. Martin. Symmetry-preserving return mapping algorithms and incrementally extremal paths: a unification of concepts. *International Journal for Numerical Methods in Engineering*, 28:1839–1853, 1989.

[16] M. Ortiz and E. P. Popov. Accuracy and stability of integration algorithms for elastoplastic constitutive relations. *International Journal for Numerical Methods in Engineering*, 21:1561–1576, 1985.

[17] A. Pérez-Foguet, A. Rodríguez-Ferran, and A. Huerta. Numerical differentiation for non-trivial consistent tangent matrices: an application to the MRS-Lade model. Submitted to *International Journal for Numerical Methods in Engineering*, 1998.

[18] D. M. Potts and A. Gens. A critical assessment of methods of correcting for drift from the yield surface in elasto-plastic finite element analysis. *International Journal for Numerical and Analytical Methods in Geomechanics*, 9:149–159, 1985.

[19] E. Pramono and K. Willam. Implicit integration of composite yield surfaces with corners. *Engineering Computations*, 6:186–197, 1989.

[20] K. Runesson and R. Larsson. Properties of incremental solutions for dissipative material. *Journal of Engineering Mechanics*, 119(4):647–666, 1993.

[21] K. Runesson, A. Samuelsson, and L. Bernspang. Numerical technique in plasticity including solution advancement control. *International Journal for Numerical Methods in Engineering*, 22:769–788, 1986.

[22] K. Runesson, S. Sture, and K. Willam. Integration in computational plasticity. *Computers and Structures*, 30(1/2):119–130, 1988.

[23] J. C. Simo and T. J. R. Hughes. *Computational inelasticity*. Springer-Verlag, 1998.

[24] J. C. Simo, J. G. Kennedy, and S. Govindjee. Non-smooth multisurface plasticity and viscoplasticity. Loading/unloading conditions and numerical algorithms. *International Journal for Numerical Methods in Engineering*, 26:2161–2185, 1988.

[25] J. C. Simo and R. L. Taylor. Consistent tangent operators for rate-independent elastoplasticity. *Computer Methods in Applied Mechanics and Engineering*, 48:101–118, 1985.

[26] S. W. Sloan and J. R. Booker. Removal of singularities in Tresca and Mohr-Coulomb yield functions. *Communications in Applied Numerical Methods*, 2:173–179, 1986.

[27] W. Squire and G. Trapp. Using complex variables to estimate derivatives of real functions. *Siam Review*, 40(1):110–112, 1998.

[28] R. S. Stepleman and N. D. Winarsky. Adaptive numerical differentiation. *Mathematics of Computation*, 33(148):1257–1264, 1979.

[29] S. Sture, K. Runesson, and E. J. Macari-Pasqualino. Analysis and calibration of a three-invariant plasticity model for granular materials. *Ingenieur Arquiv*, 59:253–266, 1989.

[30] O. C. Zienkiewicz and R. L. Taylor. *The Finite Element Method. 1 Basic formulation and linear problems*. McGraw-Hill, 4th edition, 1988.